

RSC Advances



This is an *Accepted Manuscript*, which has been through the Royal Society of Chemistry peer review process and has been accepted for publication.

Accepted Manuscripts are published online shortly after acceptance, before technical editing, formatting and proof reading. Using this free service, authors can make their results available to the community, in citable form, before we publish the edited article. This *Accepted Manuscript* will be replaced by the edited, formatted and paginated article as soon as this is available.

You can find more information about *Accepted Manuscripts* in the [Information for Authors](#).

Please note that technical editing may introduce minor changes to the text and/or graphics, which may alter content. The journal's standard [Terms & Conditions](#) and the [Ethical guidelines](#) still apply. In no event shall the Royal Society of Chemistry be held responsible for any errors or omissions in this *Accepted Manuscript* or any consequences arising from the use of any information it contains.

ARTICLE

Melatonin improves bioreductant capacity and silver nanoparticles synthesis using *Catharanthus roseus* leaves

Cite this: DOI: 10.1039/x0xx00000x

S. A. Sheshadri^a, S. Sriram^b, P. Balamurugan^a, R. Anupriya^a, S. Adline Princy^a, P. Brindha^b and S. Bindu^{*a}

Received 00th January 2012,
Accepted 00th January 2012

DOI: 10.1039/x0xx00000x

www.rsc.org/

Melatonin is a natural hormone found in a variety of living organisms, including plants, and possesses the potential to act as a growth promoter and stress alleviator. The present study aims in understanding the effect of melatonin in *Catharanthus roseus* (*C. roseus*; medicinal plant used in anticancer therapy) leaf extracts for enhanced silver nanoparticle synthesis. Our results indicated that the supplementation of 300 μM melatonin to *C. roseus* leaves improves silver nanoparticles (AgNPs) synthesis. The phytosynthesized AgNPs were characterized using UV-Vis spectroscopy, FE-TEM, Zetasizer, XRD, AAS and FTIR spectroscopy. Moreover, the AgNPs were found to be smaller in size (ranging from 10-25 nm) with potent antibacterial activity (MIC and MBC values against the most prevalent urinary tract pathogens, *Escherichia coli* and *Staphylococcus aureus*, being 15.6 ± 0.0 $\mu\text{g/ml}$ and 31.25 ± 0.0 $\mu\text{g/ml}$ respectively). Furthermore, LC-MS/MS analysis of the melatonin treated *C. roseus* leaf extracts indicated the presence of significant biomolecules; 6-acetyl morphine (used as an analgesic), rauwolscine and fisetin (anticancer compounds). Melatonin treatment of *C. roseus* leaves also enhanced its antioxidant potential and total chlorophyll content. Thus, melatonin serves as a potential agent to improve *C. roseus* growth and therapeutic potential.

Keywords: *Catharanthus roseus*, Silver nanoparticles, Melatonin

Notes and references

^a School of Chemical and Biotechnology, SASTRA University, Thanjavur, India-613401

^b Centre for Advanced Research in Indian System of Medicine, SASTRA University, Thanjavur, India-613401

*Corresponding author: Dr. Bindu Simon (bindusimon@sabt.sastra.edu)

Introduction

Melatonin (Mel; an indolic compound, N-acetyl-5-methoxytryptamine) is a well-known animal hormone and was first discovered in bovine pineal gland by Aaron Lerner as early as 1958.¹ In animals and humans, Mel functions in signalling seasonal changes, promotes immunomodulation, and also possess cytoprotective properties.¹ Though Mel was discovered in plants by 1995, much progress in unravelling the role of Mel in plants has been made possible only in the past 2 to 3 years. Mel is found to be rich in crops (rice, barley, corn, wheat and oats) and in beverages (tea, beer, wine and coffee).² Auxin, Indole-3-acetic acid (IAA) and Mel share the common biosynthetic pathway, indicating the possible coordinated regulations amongst each other. The natural antioxidant capacity of Mel might explain its ability to mitigate the toxic effect of stress in plants.^{1,3} Mel was also found to enhance the chlorophyll levels in the plant cells.⁴ Furthermore, many of the genes whose expression was altered by Mel were involved in plant stress defense.⁵ It has been suggested that Mel was involved in augmenting the levels of alkaloids in *Coffea canephora*.^{6,7} Thus Mel can act as an effective biostimulator of plant growth and defence under different environmental stress conditions.¹ Although Mel has profound documented applications in plants, its usage to enhance the therapeutic potential of medicinal plants has not been investigated till date.¹ Several medicinal plants have been known to produce bioactive compounds like alkaloids that have been effective in curing several

ailments. Plant alkaloids possess anticancer properties and are being used in pharmaceuticals.⁸ Presence of alkaloids and flavonoids as bioreducing agents in medicinal plants like *Catharanthus roseus* (*C. roseus*) have an added advantage in developing more bioavailable interventions, such as synthesis of nanoparticles.⁹

C. roseus is a well-known medicinal plant that mostly grows in tropical climates. *C. roseus* therapeutic potential has been explored for treatment of cancer and inflammation. *C. roseus* is also known to possess antimicrobial activity against a broad spectrum of microorganisms, primarily due to the presence of terpenoid indole alkaloids which impart diuretic, antidiarrhetic, anticancer, antiplasmodial, antimalarial and antiseptic properties in the plant.¹⁰⁻¹³

Plant based silver nanoparticles (AgNPs) are used as vehicles for targeted delivery of therapeutic molecules in disease treatment, mainly due to their higher surface area to volume ratio.^{13,25-29} The synthesis of AgNPs from aqueous extracts of *C. roseus* was first reported by Mukunthan et al., 2011.¹³ With nanoparticles being the new scope for targeted delivery, our research focuses on employing AgNPs from Mel treated *C. roseus* as a promising antibacterial intervention against incitants of urinary tract infections.¹³

The basis for our hypothesis corresponds to the involvement of Mel in enhancing the activity of Morphine (an alkaloid) in-vivo.^{6,7,14} Additionally, bioreduction of Ag⁺ to form AgNPs is influenced by presence of reducing compounds like flavonoids and alkaloids.¹⁵ Most of the secondary metabolites found in

Coffea canephora have been known to be enhanced by the levels of indoleamines, Mel and serotonin.

Figure 1 substantiates the role played by indolamines in alkaloids biosynthesis pathway.

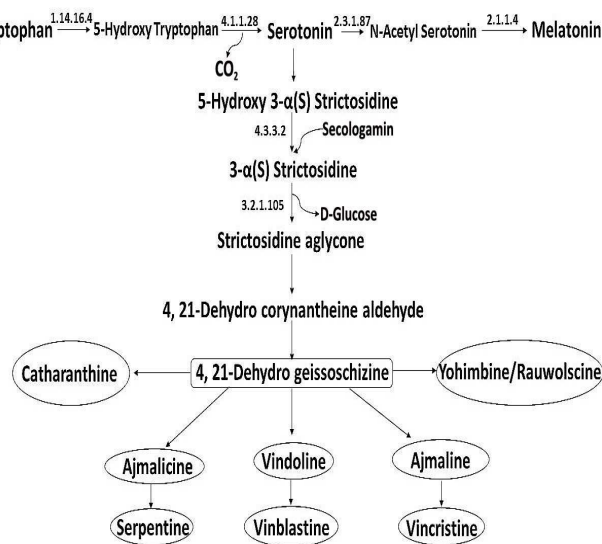


Figure 1. Indole alkaloid biosynthetic pathway (KEGG: map00901)

The present study is aimed at investigating the role of Mel in AgNPs synthesis using *C. roseus* leaf extracts as a bioreductant (using salt stress as the control for stress parameter). The selected Mel treated *C. roseus* leaf tissues were further subjected to phytochemical analysis *via* LC-MS/MS, antioxidant activity assay and chlorophyll content assay; to support our hypothesis that Mel is favourable for plant growth.¹⁶

Materials and Methods

Collection of plants and leaf feeding assay

Healthy leaves of 6 months old *C. roseus* plants were collected from the herbal garden at SASTRA university campus, Thanjavur, India. The material was washed thoroughly using tap water to ward off soil and debris and further washed twice using sterile demineralized

water. Using leaf feeding assay, *C. roseus* leaves were fed in 4 groups, first with different concentrations of Mel (10, 20, 30, 100, 200 and 300 μ M), second with 300 mM NaCl and 300 μ M Mel, third group serving as control for salt stress (300 mM NaCl only)¹⁷ and fourth group of leaflets served as water control (untreated leaves).

AgNPs synthesis

The leaf samples from all the treatment groups were deveined, trimmed and boiled in sterile merck millipore water at 80°C for 15 min. The resulting extract was filtered using Whatman no. 41 filter paper (GE healthcare, UK). AgNPs reaction mixture was prepared by mixing plant extract to 1 mM Silver Nitrate (AgNO_3 ; MM=169.87g/mol, Fisher) in the ratio of 1:10 v/v. Development of golden-brown coloration in the reaction mixture caused by reducing phyto molecules indicated the formation of AgNPs. This was further confirmed by spectroscopic analysis in the range of 200-800 nm at a resolution of 1 nm using a UV-Vis spectrophotometer (Perkin Elmer Lambda 25). The reaction mixtures that produced maximum absorbance in UV-Vis spectrum specific for AgNPs (near 440 nm)¹⁸ were used for further experiments. The selected AgNPs reaction mixture (obtained using 300 μ M Mel treated *C. roseus* leaves) was centrifuged at 10000 rpm for 12 min, and the resulting pellet was lyophilized for 2 days using freeze drier (Christ, Germany).

Characterization of AgNPs

The AgNPs were subjected to characterization by FE-TEM, Zetasizer, XRD, FTIR and AAS.

FE-TEM: To analyse the morphology of the sample, FE-TEM analysis was carried out. The sample was prepared by dispersing the AgNPs in water. A drop of the sample was placed over a carbon coated copper grid and air-dried completely at room temperature.⁴⁰ The imaging was carried out at an acceleration voltage of 200 kV using a Field emission transmission electron microscope (FE-TEM, JSM 2100F, JEOL, Japan). The images obtained were subjected to particle size analysis using ImageJ (version 1.48, National Institutes of Health, USA) and a histogram was plotted.^{40,41}

Particle size distribution analysis using Zetasizer: Size distribution of AgNPs was visualized *via* hydrodynamic diameter measurement of AgNPs dispersed in aqueous suspension through laser diffractometry using a Zetasizer (Malvern Nano ZS90, UK).^{40,41}

XRD: Crystalline nature of the sample was analysed by subjecting the sample to X-ray diffraction analysis. The freeze-dried AgNPs were coated on an XRD grid and the spectra were recorded using an X-ray diffractometer (D8 Focus, Bruker, Germany), by irradiating with Cu-K α radiation from 10⁰ to 60⁰ (2 θ) with a step size of 0.01 $^{\circ}$.

FTIR: Fourier Transform Infrared Spectra were recorded between 4000-450 cm⁻¹. The samples were prepared by following KBr pelleting using a hydraulic press. Powdered AgNPs were subjected to FTIR analysis using an FTIR spectrophotometer (Spectrum 100, Perkin Elmer, USA). This analysis allowed the identification of the possible functional groups that are responsible for the reduction of silver ion.

AAS: The sample (supernatant from AgNPs reaction mixture) was assayed for the unreacted elemental silver using an Atomic Absorption Spectrometer

(AAnalyst400, Perkin Elmer USA). The concentration value thus obtained was subtracted from the initial concentration of Ag⁺ (1 mM) to calculate the amount of silver that participated in AgNPs formation. The result was expressed in mg/L.

Antimicrobial activity assay

The minimum inhibitory concentration (MIC) and minimum bactericidal concentration (MBC) were determined by the broth micro dilution method in microtitre plate. AgNPs (derived from 300 μ M Mel treated *C. roseus* leaves) were adjusted to a stock concentration of 500 μ g/ml using LB media and the next two fold dilution of the initial concentration was carried out till 3.5 μ g/ml. Optical density (OD) of overnight grown cultures of the clinical uropathogenic isolates, *Escherichia coli* and *Staphylococcus aureus* were adjusted to 10⁶-10⁷ cfu/mL. 10 μ l of the culture was inoculated in 200 μ l of media containing AgNPs and the plates were incubated at 37 $^{\circ}$ C, stationary for 24 h. The growth of bacteria was monitored by measuring the OD at 600 nm at the end of 24 h. MIC was described as the concentration that caused complete inhibition of growth of bacteria. 100 μ l of the culture was centrifuged; pellet was washed in 1X PBS and resuspended in 100 μ l of 1X PBS. The pellet suspension was spread plated onto LB agar plates. Standard antibiotic Gentamicin (20 μ g/ml) was used as the control for antibiotic susceptibility. Culture wells without the AgNPs or Gentamycin served as positive control. The concentration at which no colonies appeared on agar plates was described as MBC. All the experiments were carried out in triplicates and percentage growth was calculated using the formula:

$$\% \text{ Growth} = [\text{Test} / \text{Positive control}] \times 100$$

LC-MS/MS analysis

Phytochemical screening of the untreated (control) and 300 μM Mel treated *C. roseus* leaf extracts were carried out using LC-MS/MS analysis (UHPLC Dionex C18 RP Acclaim 120 Å, 2.1 \times 150 mm, 3.0 μm column, USA and MSMS Bruker Q-II TOF). LC was carried out at 355 nm, 0.2 mL/min flow rate, gradient mobile system started with 94% A to 80% A (Acetonitrile acidified with acetic acid) in 1 min and maintained to 80% for next 4 min. This was then brought to 5% at 15th min. MS was carried out by Electro Spray Ionization (ESI), Nebulizer pressure-24.7 psi with 6.0 l/min N_2 flow, m/z range: 50-1000 m/z, Capillary voltage - 3000 V, dry heater temperature at 280 °C. Mass spectrometry data was obtained in the negative and positive ionization modes.

Chlorophyll quantification

The untreated and 300 μM Mel treated *C. roseus* leaves were subjected to chlorophyll analysis using method of Porra, 2002.¹⁹ 50 mg of fresh leaves from each sample were crushed by adding liquid nitrogen, ground in 10 ml N,N-dimethylformamide (DMF) in an orbital shaker for 2 h and then centrifuged at 4000 g for 20 min. Absorbance of the supernatant was measured at 663.8 nm and 646.8 nm. Total chlorophyll concentrations per unit leaf fresh weight ($\mu\text{g/g}$) were calculated using extinction coefficients and simultaneous equations for DMF extraction derived by Porra, 2002.¹⁹

$$\text{Total chlorophyll content [chl a+b]} = 17.67 (E^{647}) + 7.12 (E^{664})$$

Antioxidant activity assay

The DPPH (2,2-diphenyl-1-picrylhydrazyl) radical scavenging activity was also analysed for the untreated

and 300 μM Mel treated *C. roseus* leaves following Sanchez-Moreno et al., 1998 method.²⁰ The extract (100 μl) was added to 3.9 ml of DPPH methanolic solution (0.025 g/L) and the reactants were incubated at 25 °C for 30 min. Different concentrations of quercetin was used as reference standard and methanol was used as the negative control. The decrease in absorbance was measured at 515 nm using a microplate spectrophotometer (Epoch, BioTek Instruments Inc., USA). The radical scavenging activity of tested samples was calculated and expressed on percentage basis using the formula:

$$\text{DPPH radical scavenging activity} = (\text{Abs of control} - \text{Abs of sample} / \text{Abs of control}) \times 100$$

The graphs and statistical analysis for the required data were carried out using GraphPad Prism version 5.04 (GraphPad Prism software Inc. USA).

Results and Discussion

AgNPs synthesis was found to be higher for 300 μM Mel treated *C. roseus* leaves when compared to the untreated leaves. This was evidenced by the golden brown colour of the reaction mixture and the UV-Vis spectroscopy peak at 440 nm (Figure 2A and 2B). This outcome substantiated the enhancing potential of Mel in AgNPs synthesis. Generally surface plasmon resonance peak for AgNPs is found within the range of 400-450 nm.^{13,21} The reaction mixtures containing other concentrations of Mel (data not shown) or 300 mM NaCl and 300 μM Mel or 300 mM NaCl, produced no peaks (as seen in Figure 2B); indicating the negative impact of salt stress in AgNPs synthesis. Despite the golden brown coloration in the AgNPs reaction

mixtures containing 300 mM NaCl and 300 μ M Mel, the corresponding peak at 440 nm was found to be absent, signifying undetectable levels of AgNPs synthesis in presence of salt stress.

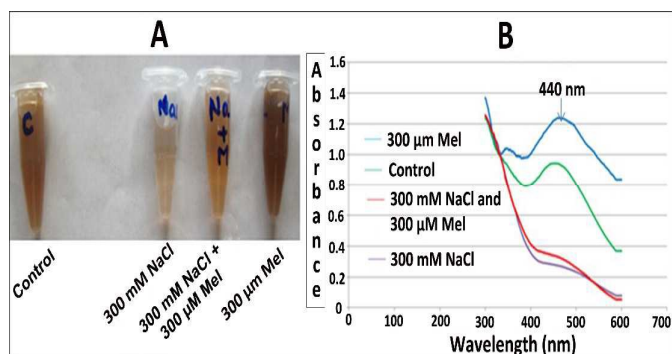


Figure 2. Effect of Mel on AgNPs synthesis using *C. roseus* leaf extracts. A. The picture shows AgNPs reaction mixtures prepared by mixing leaf extracts from different samples [leaves treated with either water (control); 300 mM NaCl; 300 mM NaCl and 300 μ M Mel; 300 μ M Mel] with 1 mM AgNO₃, in the ratio of 1:10 v/v, followed by incubation for 48 h in dark at room temperature. B. UV-Vis spectroscopy results for the respective AgNPs reaction mixtures (analysed in the range of 200-800 nm at a resolution of 1 nm).

The AgNPs derived from 300 μ M Mel treated *C. roseus* leaves were characterised using FE-TEM, Zetasizer, XRD, FTIR and AAS. The morphology and size of AgNPs analysed by FE-TEM depicted spherical shaped AgNPs having particle size varying from 10-25 nm (Figure 3). The FE-TEM images were analysed by ImageJ software and the resultant size distribution histogram is shown in Figure 4. The average size of AgNPs derived from *C. roseus* leaves were reported differently by various researchers and were found in the ranges 27-32 nm¹⁰, 48-67 nm¹³ and 35-55 nm¹¹, present characterization yielded relatively smaller AgNPs, with a better potential for delivery of vital biomolecules.¹³

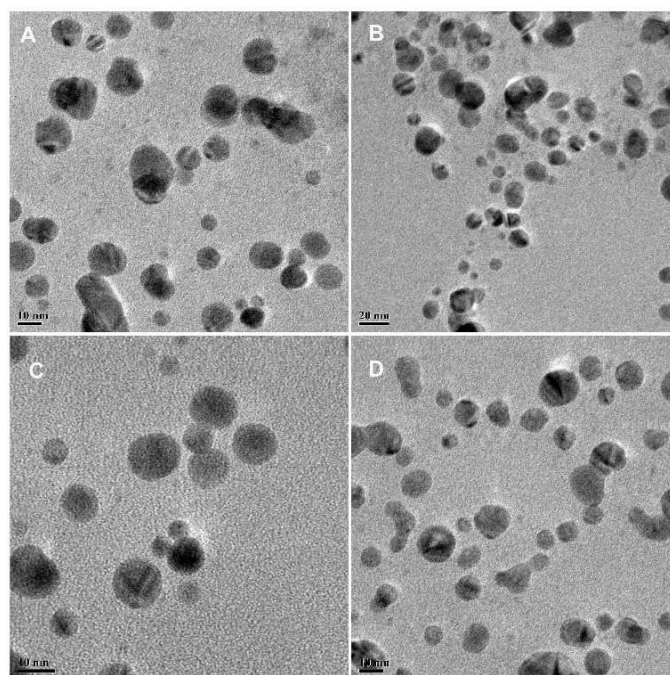


Figure 3. FE-TEM analysis showing presence of AgNPs in the size range of 10-25 nm (Image A,C,D: 10 nm scale; Image B: 20 nm scale)

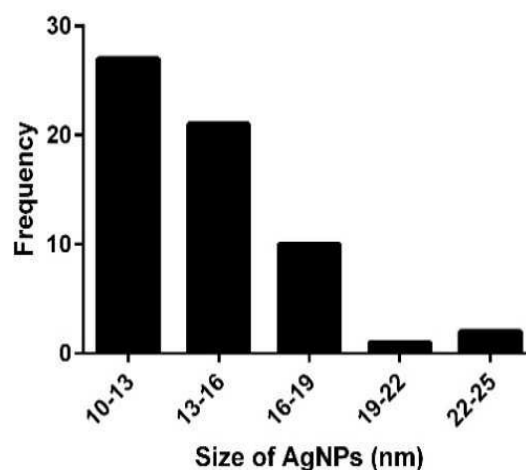


Figure 4. Size distribution of AgNPs using ImageJ V1.48

Particle size assessment performed using Zetasizer estimated the average hydrodynamic diameter of AgNPs as 180.8 nm, and the polydispersion index was found to be 0.438 (Figure 5). The difference in the size of AgNPs ascertained *via* FE-TEM (10-25 nm) and

Zetasizer (180.8 nm) is consistent with the previous literatures.^{40,41}

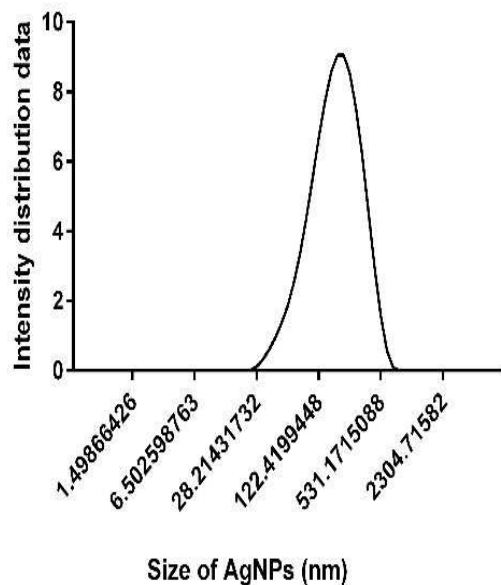


Figure 5. Particle size analysis using Zetasizer

XRD analysis offered details regarding the crystalline nature of the AgNPs. Freeze-dried AgNPs synthesized from Mel treated leaf extracts showed characteristic diffraction pattern with peaks at 27.315° , 31.874° , 37.698° indexed to the (210), (122), (123) crystalline planes (Figure 6). Similar XRD patterns for the green synthesized AgNPs have been reported by various researchers, additionally illustrating their crystalline nature.^{13,22,23} Additional and unmapped peaks were also observed in the spectra, pointing to the presence of other organic substances in the sample. The line broadening of the peaks is attributed primarily to the small particle size of AgNPs.³⁹

Owing to the presence of several bioreducing agents in the extract of 300 μ M Mel treated *C. roseus* leaves; it is arduous to ascertain the exact identity of biomolecules

that cause the reduction of Ag^+ to form AgNPs. However using FTIR results, the potential bioreducing and capping agents were identified by mapping the peaks to the standard designated peaks.

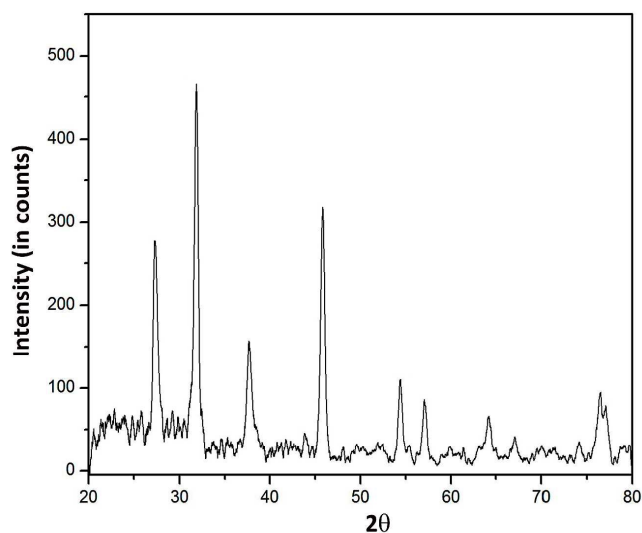


Figure 6. XRD profile of AgNPs depicting peaks at 27.315° , 31.874° , 37.698° (2θ)

The peak observed at 3401.2 cm^{-1} indicated the stretching of O-H bond present characteristically among alcohols and phenols. The peak observed at 1604.11 cm^{-1} corresponds to amide-I band arising out of C=O stretch, exhibited mostly by flavonoids and alkaloids. The peak at 1384.59 cm^{-1} coincides with C-H stretching, mapped to the presence of methyl groups. The comparatively smaller peak observed at 1071.02 cm^{-1} could be mapped to C-N stretching, observed among amines.²¹⁻²³ Hence, it can be assumed that these biomolecules are potentially responsible for capping and stabilization of the AgNPs. The FTIR spectra are shown in Figure 7.

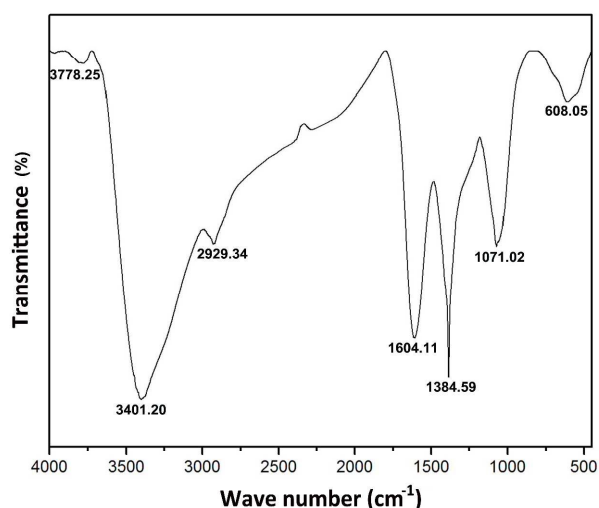


Figure 7. FTIR spectrum for AgNPs showing characteristic peaks at 3401.2, 1604.11, 1384.59 and 1071.02 cm^{-1}

The AAS analysis led to the estimation of the silver content in the supernatant of AgNPs reaction mixture as 21.908 mg/L. Since 1 mM AgNO_3 was employed in the AgNPs synthesis, the approximate quantity of silver that was involved in AgNPs synthesis was estimated to be 86.09 mg/L.

The biosynthesized AgNPs (using 300 μM Mel treated *C. roseus* leaves) showed potent activity against the urinary tract pathogens, *Escherichia coli* and *Staphylococcus aureus*, with an MIC value 15.6 ± 0.0 $\mu\text{g/ml}$ and an MBC value 31.25 ± 0.0 $\mu\text{g/ml}$. The Figure 8 shows the percentage growth of the tested cultures under various concentrations of AgNPs. There have been several investigations conducted in order to test the antimicrobial potential of AgNPs using different modes of synthesis. AgNPs derived from chemical reduction method have reported an MIC value of 100 $\mu\text{g/ml}$ against *Staphylococcus aureus* and *Escherichia coli*²⁵ while those derived *via* green synthesis route

from known medicinal plants have shown varied values of MIC; like *C. roseus* (MIC value of 1000 $\mu\text{l/ml}$ against *Bacillus subtilis*, *Staphylococcus aureus*, *Escherichia coli*, *Klebsiella pneumonia* and *Candida albicans*²⁶ and 40 $\mu\text{g/ml}$ against *Escherichia coli*, *Pseudomonas aeruginosa*, *Bacillus subtilis* and *Staphylococcus aureus*²⁷), *Garcinia mangostana* (MIC value of 20 $\mu\text{g/ml}$ against *Staphylococcus aureus* and *Escherichia coli*)²⁸ and *Acalypha indica* (MIC value of 10 $\mu\text{g/ml}$ against *Escherichia coli* and *Vibrio cholerae*).²⁹ We can infer through our investigation that AgNPs derived from Mel treated *C. roseus* leaves are better antibacterial agents (with an MIC value of 15.6 ± 0.0 $\mu\text{g/ml}$ as compared to the existing literary evidences^{26,27}) against uropathogenic isolates (*Escherichia coli* and *Staphylococcus aureus*).

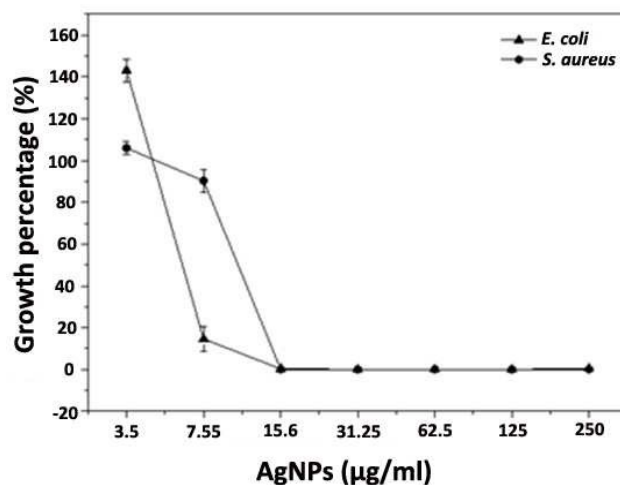


Figure 8. Antibacterial activity of AgNPs against uropathogens

Metabolite profiling by LC-MS/MS yielded several compounds that were found to be common in untreated and 300 μM Mel treated *C. roseus* leaves. These commonly found compounds have been enlisted in Table 1, and their respective MS/MS spectra

ARTICLE

have been depicted in supplementary Figure 1. It was observed that 6-acetylmorphine, rauwolscine and fisetin were found exclusively in the spectrum of 300 μM Mel treated *C. roseus* leaves (Table 2 and supplementary Figure 2). While rauwolscine (an alkaloid that is most commonly found in *Rauwolfia* species) has been found to possess anticancer, antioxidant and antiinflammatory potential,³⁰ fisetin (a flavonoid) is known to possess antitumor properties against various types of cancers in humans, along with antioxidant and antimicrobial potential.³⁰ Additionally, 6-acetylmorphine (a mammalian peripheral-to-central hormone) has better potency of penetration than morphine, in-vivo. It is also used as an analgesic.³¹ As a significant observation, these three compounds were not reported in the aqueous extracts of untreated leaves of *C. roseus*, reinforcing our hypothesis that 300 μM Mel has an effect in altering the metabolite profile of aqueous extract of *C. roseus* leaves.

Chlorophyll content of the Mel treated *C. roseus* leaves were significantly higher ($81.31 \pm 2.45 \mu\text{g/ml}$) than the untreated leaves ($33.39 \pm 1.83 \mu\text{g/ml}$), as seen in Figure 9. Researchers have shown similar results in other plant systems.^{4,35} Since there is a positive correlation between chlorophyll levels and photosynthetic activity,³⁶ Mel may have an indirect role in enhancing the photosynthetic activity in plants.

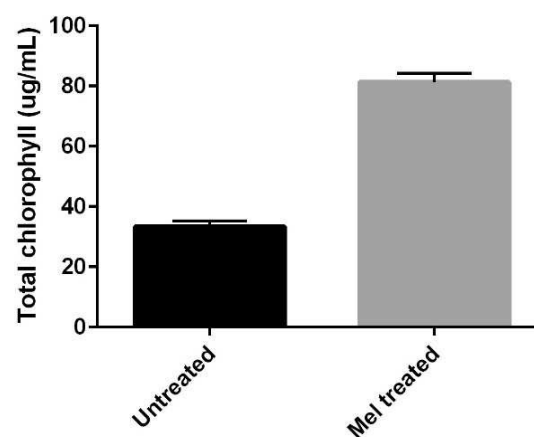


Figure 9. Increase in the total chlorophyll content in Mel treated (300 μM) vs untreated *C. roseus* leaves

| S. No. | R.T (min) | Compound | [M+H] | [M-H] | MS/MS (Product ion) | Reference |
|--------|-----------|---------------|-------|-------|---------------------|-----------------------------------|
| 1 | 0.1-0.2 | Catharanthine | 337.2 | - | 320,144 | 32,33 |
| 2 | 0.9-1.0 | Camptothecin | 349.2 | - | 168,206,218 | 34, Mass bank database (BML00417) |
| 3 | 4.0-4.1 | Vindolinine | 337.1 | - | 320,308,276 | 32,33 |
| 4 | 13.6-14.0 | Vindoline | 457.3 | - | 397,188 | 32 |
| 5 | 14.9 | Amorphigenin | 411.2 | - | 179,188 | Mass bank database (BML00192) |

Table 1. Common compounds in untreated and Mel treated (300 μM) *C. roseus* leaves (R.T: Retention time)

| S. No. | R.T (min) | Compound | [M+H] | [M-H] | MS/MS (Product ion) | Reference |
|--------|-----------|------------------|-------|-------|---------------------|-------------------------------|
| 1 | 6.0-6.4 | 6-Acetylmorphine | 328.2 | - | 211,193,165 | Mass bank database (WA002835) |
| 2 | 9.6-9.9 | Rauwolscine | 355.2 | - | 144, 163,194,248 | Mass bank database (BML00496) |
| 3 | 10.9 | Fisetin | - | 285.2 | 153,163,195,242 | Mass bank database (FIO00093) |

Table 2. Unique compounds in Mel treated (300 μM) *C. roseus* leaves (R.T: Retention time)

ARTICLE

DPPH radical scavenging activity resulted in a percentage inhibition value of $76.760 \pm 0.04\%$ for 300 μM Mel treated *C. roseus* leaves on par with $57.906 \pm 0.01\%$ for untreated ones, while quercetin control showed a DPPH inhibition at $78.826 \pm 0.28\%$. A one-way ANOVA test was performed to quantify the significance of the DPPH inhibition values. With a p -value of <0.0001 , the means showed significant differences, thus Mel treated *C. roseus* leaves showed significantly higher antioxidant activity than its untreated counterpart (as seen in Figure 10). Augmenting effects of Mel treatment on antioxidant properties of plant leaves have been reported by several researchers,^{4,35} with focus on cytoprotective activity and our results further substantiate them. Higher antioxidant potential has been found to protect the plants from abiotic stress situations.⁴

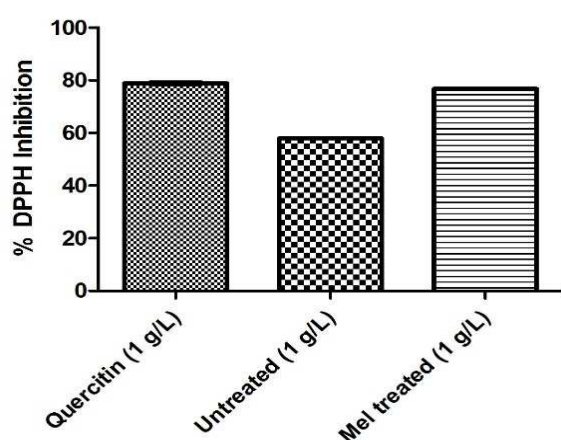


Figure 10. DPPH antioxidant activity for Quercetin (reference standard); untreated versus Mel treated (300 μM) *C. roseus* leaves

Conclusion

Our studies were streamlined in determining the role of Mel in the medicinally significant plant, *C. roseus*. The studies conducted showed a positive correlation between Mel supplementation (300 μM) and AgNPs synthesis. The AgNPs synthesized using Mel treated *C. roseus* leaves had properties characteristic for AgNPs, as evidenced by UV-Vis spectroscopy, FE-TEM, Zetasizer, XRD, AAS, and FTIR analysis. The synthesized AgNPs were found to be smaller in size (10-25 nm) in comparison to the untreated *C. roseus* leaves (27-55 nm),^{10,13,11} and also possessed the crystalline properties characteristic to AgNPs. The AgNPs showed potent antibacterial activity against urinary tract pathogen isolates (*Escherichia coli* and *Staphylococcus aureus*); with an MIC value of $15.6 \pm 0.0 \mu\text{g/ml}$ and an MBC value of $31.25 \pm 0.0 \mu\text{g/ml}$. Thus, the AgNPs derived from Mel treated *C. roseus* leaves were found to be better antimicrobial agents than those produced via green synthesis from other medicinal plants.²⁶⁻²⁹ Our results also indicated that 300 μM Mel supplementation to *C. roseus* leaves (the concentration that improved AgNPs synthesis) had a profound impact on the metabolites, leading to the detection of anticancer compounds, fisetin and rauwolscine, as well as the anti-inflammatory compound, 6-acetyl morphine. In addition, 300 μM Mel feeding to *C. roseus* leaves also improved the total chlorophyll content and antioxidant potential. Thus, our data endorses that Mel augments

the therapeutic potential of the medicinal plant *C. roseus*.

Acknowledgements

The authors are thankful to SASTRA University for providing TRR in-house funding, as well as necessary infrastructure and facility to carry out the experiments. We are grateful to Mr. K. Balaji for carrying out the TEM analysis.

References

- 1 K. M. Janas, M. M. Posmyk, *Acta Physiol. Plant*, 2013, **35**, 3285-3292
- 2 D. X. Tan, R. Hardeland, L. C. Manchester, A. Korkmaz, S. Ma, S. Rosales-Corral, R. J. Reiter, *J. Exp. Bot.*, 2011, **63**, 577-597
- 3 K. Szafrńska, S. Glińska, K. M. Janas, *Biologia Plantarum*, 2013, **57**, 91-96
- 4 M. B. Arnao, *Adv. Bot.*, 2014, **2014**, 1-11
- 5 S. Weeda, N. Zhang, X. Zhao, G. Ndip, Y. Guo, G. A. Buck, C. Fu, S. Ren, *Plos One*, 2014, **9**, 1-18
- 6 A. Ramakrishna, P. Giridhar, G. A. Ravishankar, *Plant Signal Behav.*, 2011, **6**, 800-809
- 7 A. Ramakrishna, P. Giridhar, K. U. Sankar, G. A. Ravishankar, *Acta Physiol. Plant*, 2012, **34**, 393-396
- 8 A. Veloso, B. Biewen, M. T. Paulsen, N. Berg, L. C. de Andrade Lima, J. Prasad, K. Bedi, B. Magnuson, T. E. Wilson, M. Ljungman, *Plos One*, 2013, **8**, 1-10
- 9 M. Magnotta, J. Murata, J. Chen, V. De Luca, *Phytochem.*, 2006, **67**, 1758-64
- 10 V. S. Kotakadi, Y. S. Rao, S. A. Gaddam, T.N.V.K.V. Prasad, A. V. Reddy, D.V.R. S. Gopal, *Colloids and surfaces. B, Biointerfaces*, 2013, **105**, 194-8
- 11 S. Ponarulselvam, C. Panneerselvam, K. Murugan, N. Aarthi, K. Kalimuthu, S. Thangamani, *Asian Pac. J. Trop. Biomed.*, 2012, **2**, 574-580
- 12 S. Gurunathan, J. W. Han, D. N. Kwon and J. H. Kim, *Nanoscale res lett.*, 2014, **9**, 373
- 13 K. S. Mukunthan, E. K. Elumalai, T. N. Patel, V. R. Murty, *Asian Pac. J. Trop. Biomed.*, 2011, **1**, 270-274
- 14 N. Y. F. Abadi, P. T. Fahadan, K. Riazi, M. H. Ghahremani, A. R. Dehpour, *Epilepsy Res.*, 2007, **75**, 138-144
- 15 A. Soni, S. Sosa, *J Pharmacogn Phytochem.*, 2013, **2**, 22-29
- 16 P. Wang, X. Sun, C. Li, Z. Wei, D. Liang, F. Ma, *J. Pineal Res.*, 2013, **54**, 292-302
- 17 A. H. M. A. Mohammed, *Res. J. Agri. Biol. Sci.*, 2007, **3**, 200-213
- 18 A. M. Awwad, N. M. Salem, A. O. Abdeen, *Int. J. Ind. Chem.*, 2013, **4**, 29
- 19 R. J. Porra, *Photosynth. Res.*, 2002, **73**, 149-156
- 20 C. S. Moreno, J. A. Larrauri, F. S. Calixto, *J. Sci. Food Agric.*, 1998, **76**, 270-276
- 21 M. M. H. Khalil, E. H. Ismail, K. Z. El-Baghdady, D. Mohamed, *Arabian J. Chem.*, 2014, **7**, 1131-1139
- 22 T.Y. Suman, S. R. R. Rajasree, A. Kanchana, S. B. Elizabeth, *Colloids and Surfaces B: Biointerfaces*, 2013, **106**, 74-78
- 23 A. A. Zahir, A. A. Rahuman, *Veterinary Parasitol.*, 2012, **187**, 511-520
- 24 U. Kim, S. B. Han, O. S. Kwon, H. H. Yoo, *Mass Spectrom. Lett.*, 2011, **2**, 20-23

- 25 K. Soo-Hwan, H. S. Lee, D. S. Ryu, S. J. Choi, D. S. Lee, *Korean J. Microbiol. Biotechnol.*, 2011, **39**, 77-85
- 26 R. B. Malabadi, R. K. Chalannavar, N. T. Meti, G. S. Mulgund, K. Nataraja, S. V. Kumar, *Res. Pharm.*, 2012, **2**, 18-31
- 27 M. B. Prakash, S. Paul, *Int. J. Appl. Biol. Pharm. Tech.*, 2012, **3**, 105-111
- 28 R. Veerasamy T. Z. Xin, S. Gunasagaran, T. F. W. Xiang, E. F. C. Yang, N. Jeyakumar, S. A. Dhanaraj, *J. Saudi Chem. Soc.*, 2011, **15**, 113-120
- 29 C. Krishnaraj, E. G. Jagan, S. Rajasekar, P. Selvakumar, P. T. Kalaichelvan, N. Mohan, *Colloids and Surfaces B: Biointerfaces*, 2010, **76**, 50-56
- 30 A. Parsaeimehr, E. Sargsyan, A. Vardanyan, 2011, *ABAH Bioflux*, **3**, 115-124
- 31 C. J. Weitz, L. I. Lowney, K. F. Faull, G. Feistner, A. Goldstein, *Proc. Natl. Acad. Sci.*, 1988, **85**, 5335-5338
- 32 Q. Chen, W. Zhang, Y. Zhang, J. Chen, Z. Chen, *Food Chem.*, 2013, **139**, 845-852
- 33 F. Ferreres, D. M. Pereira, P. Valentão, J. M. A. Oliveira, J. Faria, L. Gaspar, M. Sottomayor, P. B. Andrade, *J. Pharm. Biomed. Anal.*, 2010, **51**, 65-69
- 34 S.C. Puri, G. Handa, B.A. Bhat, V.K. Gupta, T. Amna, N. Verma, R. Anand, K.L. Dhar, G.N. Qazi, *J. Chromatogr. Sci.*, 2005, **43**, 348-350
- 35 M. B. Arnao, J. Hernandez-Ruiz, *J. Pineal Res.*, 2009, **46**, 58-63
- 36 C. C. Black Jr., M. C. Mayne, *Plant Physiol.*, 1970, **45**, 738-741
- 37 C. Yi, Y. Zhang, Z. Yu, Y. Xiao, J. Wang, H. Qiu, W. Yu, R. Tang, Y. Yuan, W. Guo. W. Deng, *Plos One*, 2014, **9**, 1-11
- 38 W. Wei, Q. T. Li, Y. Chu, R. J. Reiter, X. M. Yu, D. H. Zhu, W. K. Zhang, B. Ma, Q. Lin, J. S. Zhang, S. Y. Chen, *J. Exp. Biol.*, 2014, 1-13
- 39 V. S. Vinila, R. Jacob, A. Mony, H. G. Nair, S. Isaac, S. Rajan, A. S. Nair, J. Isac, *Crystal Structure Theory and Applications*, 2014, **3**, 1-9
- 40 Z. Yu, M. Yu, Z. Zhang, G. Hong and Q. Xiong, *Nanoscale Res Lett*, 2014, **9**, 343, 1-7
- 41 T. Wagner, H. G. Lipinski, M. Wiemann, *J. Nanopart Res*, 2014, **16**, 2419, 1-10